ORGANIC PROCESS RESEARCH & DEVELOPMENT
OPR&D



Full Paper

# An efficient multigram synthesis of hypericin improved by a low power LED based photoreactor

Renato Sonchini Gonçalves, Bruno Ribeiro Rabello, Gabriel Batista Cesar, Paulo C. S. Pereira, Marcos Alessandro dos Santos Ribeiro, Eduardo C. Meurer, Noboru Hioka, Celso Vataru Nakamura, Marcos Luciano Bruschi, and Wilker Caetano

*Org. Process Res. Dev.*, **Just Accepted Manuscript** • Publication Date (Web): 28 Nov 2017



ACS Publications

Organic Process Research & Development is published by the American Chemical Society. 1155 Sixteenth Street N.W., Washington, DC 20036

# An efficient multigram synthesis of hypericin improved by a low power LED based photoreactor

*Renato S. Gonçalves*[*†], *Bruno R. Rabello*[‡], *Gabriel B. César*[†], *Paulo C. S. Pereira*[†], *Marcos A. S. Ribeiro*[†], *Eduardo C. Meurer*[‖], *Noboru Hioka*[†], *Celso V. Nakamura*[§], *Marcos L. Bruschi*[§] *and Wilker Caetano*[†]

[†] Department of Chemistry, State University of Maringá, Avenue Colombo, 5790, Maringá, Paraná, 87020-900, Brazil.

[‡] Instituto Federal de Educação, Ciência e Tecnologia Catarinense, 283, Concórdia, Santa Catarina, 89703-720, Brazil.

[§] Department of Pharmacy, State University of Maringá, Avenue Colombo, 5790, Maringá, Paraná, 87020-900, Brazil.

[‖] Federal University of Parana, Jandaia do Sul, Paraná, 86900-000, Brazil.

**ABSTRACT**: In this work, an improved synthesis process was developed for the multigram production of hypericin. An inexpensive and efficient low power Light Emission Diode (LED) based photoreactor was designed and employed to perform the protohypericin photocyclization reaction allowing its photoconversion in hypericin. This closed system overcomes safety issues related to scale-up hypericin preparation typically described in the literature which combine the

use of open systems, organic solvents and high-power light sources. The photoreactor designed allow to solve mainly the intrinsic effect of hypericin photobleaching inherent to protohypericin photocyclization reaction, implying in the yield increased of the final product and consequently in the final cost. Using a red LED based photoreactor a safety protocol was carried out to 5-gram scale hypericin preparation with quantitative yield.

**KEYWORDS**: Hypericin synthesis, LED, photoreactor, photobleaching effect, photocyclization reaction, electronic absorpition spectroscopy, kinetic studies, gram-scale.

## INTRODUCTION

Hypericin is a naturally occurring naphtodianthrone found in plants of the genus Hypericum, commonly known as Saint John's Wort.[1] Hypericin have attracted increasing attention due to broad spectrum of pharmacological applications, among which anti-depressive, antiviral, anti-inflammatory, and anti-tumoural activities have been reported.[2-4] However, the difficulty in obtaining hypericin in both significant amount and pure state direct from plant material imply in its very higher commercial cost (1 mg ~ 95%, USD 815.81), unfeasibly its utilization on large-scale. In order to overcome this limitation, different synthetic routes have been proposed for hypericin including the first total synthesis comprising a 12 process steps, starting from 3,5-dimethoxyphtalic anhydride and m-cresol.[5-12] One year later, the synthesis of hypericin was accomplished by a semi-synthetic route starting from emodin anthrone, which is converted to emodin bianthrone by an oxidative dimerization process followed by a base-catalyzed oxidation to protohypericin and finally exposure to bright sunlight to yield hypericin with a low yield of 10%.[13] This semi-synthetic strategy was later adapted by Steglish et al. and adopted by others.[14-16] Starting from emodin, the procedure consist in a reductive coupling by a 3 week long

treatment with alkali and hydroquinone to obtained protohypericin, which after workup was irradiated with sunlight to obtained hypericin in 29% yield.

In 1998, Mazur et al. improved this semi-synthetic route employing an oxygen transfer reagent (pyridine N-oxide) and a conventional redox catalyst for the oxidative dimerization of emodin to protohypericin. The photocyclization reaction of protohypericin was carried out with employed of halogen lamp (500 W), which after a prolonged irradiation time yielded 60% of hypericin.[17] Interestingly, in the works reported later concerning the synthesis of hypericin and its derivatives, were described the use of high-power (400-1000 W) and multifrequential light sources in the photocyclization step.[18-29] Moreover, as far as we know, none of these works considers the possibility of the hypericin photobleaching effect when the photocyclization step is conducted under uncontrolled experimental conditions.[30,31] The photobleaching effect is characterized by photochemical changes on dyes molecular structure resulting of covalent bonds disruption, which are integrant of chromophore and fluorophore groups. As a result of this chemical disruption, the dye loses its characteristic color and/or its ability to emit fluorescence for instance.[25] As such, the present case concerning the hypericin formation whose electronic absorption spectral show an expressive overlapping with the emission spectral of the light source, the photobleaching effect is relatively pronounced. Therewith, the low hypericin yield associated with its photobleaching effect and induced by the use of high-power and multifrequential light source can impact mainly on its large-scale production cost. Therefore, these are factors of great study interest, in the sense of seeking alternatives for the minimization of the physic-chemical and photophysical parameters that may induce the photobleaching process in these systems. In this work, we show that the overall yield of hypericin synthesis provided by preceding works can be significantly improved if the protohypericin

photocyclization reaction is performed under low-power Light Emission Diode (LED) sources that show well-defined spectral irradiance bands. Here, we described the design and application of a LED based photoreactor to improve the multi-gram scale preparation of hypericin. Specifically, our project is applied in the protohypericin photoconversion reaction, the final step of the hypericin synthesis. Our project brings together innovative factors from earlier designs: (i) The substitution of relative high-power light sources (Watt) by low-power LEDs light sources (mW); (ii) A compact and transparent flow cell in zig-zagging format maximizing the exposure of the circulating sample to the radiation flux; (iii) A vertically mounted system in modular units allowing an adjustment of the specific light dose ($mW/cm^2$) and reaction time based on the initial amount of reagent; (iv) Controlled recirculation of the reagent into the flow cell ensuring a maximum protohypericin photoconversion (v) Coupling of an optical fiber to the output of the sample stream, interfaced to an analysis device. All those parameters adjusted allow to optimized the protohypericin photoconversion step, reducing the temporal exposure of hypericin to specific light irradiation with relative low-power light dose, simultaneously modulating the photoreaction and minimizing the photoinduced processes that lead to its photodegradation. Among the advantages of our design is the fact that the photocyclization reaction can be performed in a closed system, overcomes safety issues related to scale-up hypericin preparation typically described in the literature which combine the use of open systems, organic solvents and high-power light sources.

## RESULTS AND DISCUSSION

**Photoreactor Design.** The prototype LED based photoreactor described in this study was comprised by at least four or more photo-reactive modular units vertically arranged in series. The modular unit consist of a three-bay aluminum chassis (10 x 20 x 8 cm) supported by a multiple heat sink cooling system. In the central bay is inserted the flow cell, which is consists of a transparent Pyrex tube in zig-zagging format (3 mm intern diameter, 180 cm length). In both faces of the modular unit sits two irradiation systems, composed by six LEDs blocks of 3.0 x 4.5 $cm^2$. Each LEDs block consists of 36 x red 1210-SMD (Surface Mounted Diode) LEDs of light dose 12.5 $mW/cm^2$ (with a maximum emission at 530 nm), positioned at 1.0 cm and parallel from flow cell (Figure 1). For supply the protohypericin solution into photoreactor, the bottom of the photoreactor is equipped with a Supelco PEEK fitting that attaches to 1/16" tubing that connects to a metering pump. The protohypericin solution is pumped from feed flask (amber glass) into the flow cell by down of the photoreactor. The flow rate of the metering pump can be adjusted based on the initial concentration of reagent solution (protohypericin). At the top of the photoreactor is fitted with a Supelco PEEK fitting that attaches to 1/16" tubing that connects to a micro-splitter valve interfaced to a spectrophotometer and equipped with a continuous flow quartz cuvette. The control valves allow to adjust the sample input on the spectrophotometer and recirculate the reagent into the flow cell until its total photoconversion in hypericin. The S40 thread adaptors at the feed and collection flasks provide necessary air ($O_2$) to be mixed with the reagent solution before get in to the flow cell.

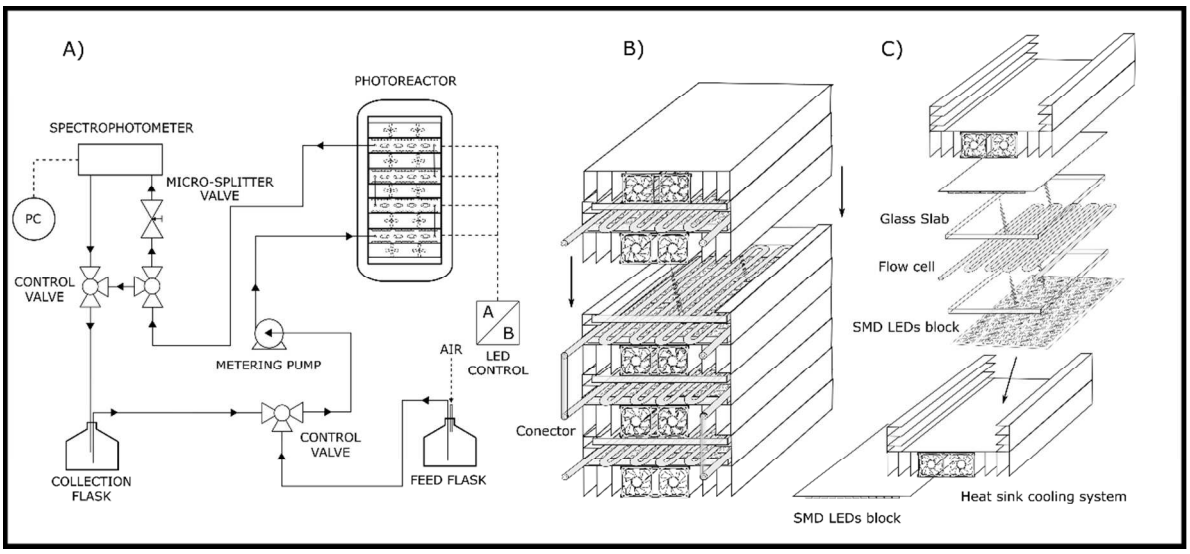


Figure 1. (A) Process flow diagram of the protohypericin photoconversion. (B) Showing the photoreactor vertically arranged with four photo-reactive modular units interlocked. (C) Showing the deconstructed modular unit. The flow cell is inserted between two glass slabs preventing the intimate contact of the sample with the irradiation systems.

**Synthesis of Hypericin.** Naphtodianthrone hypericin was synthesized through adapted literature procedures employing the emodin as starting material (Scheme 1).[17-19] Significant amount of emodin was accessed reproducing the optimized protocol for the isolation of anthraquinones from *Cortex Frangula*.[34] Briefly, dry bark of stem and branches of *Rhamnus frangula* L. was tritured and macerated in MeOH at room temperature. The extracts were concentrated, hydrolysed in acid medium and exhaustively extracted with DCM in a Soxhlet apparatus. Isolation of anthraquinones from crude extract was performed by silica gel column chromatography employed a mixture of $CHCl_3$ : AcOEt with a gradient of 0-15% as mobile phase. Elution with an increase of the solvent polarity (addition of 15% AcOEt) provide an eluate of orange color. TLC analysis revealed that the fractions correspondent to its eluate were sufficiently purified, and the isolated emodin (≥ 98%) was confirmed by $^1$H NMR analyse (Figures S7 and S8).

Scheme 1. Optimized experimental conditions for the hypericin synthesis.

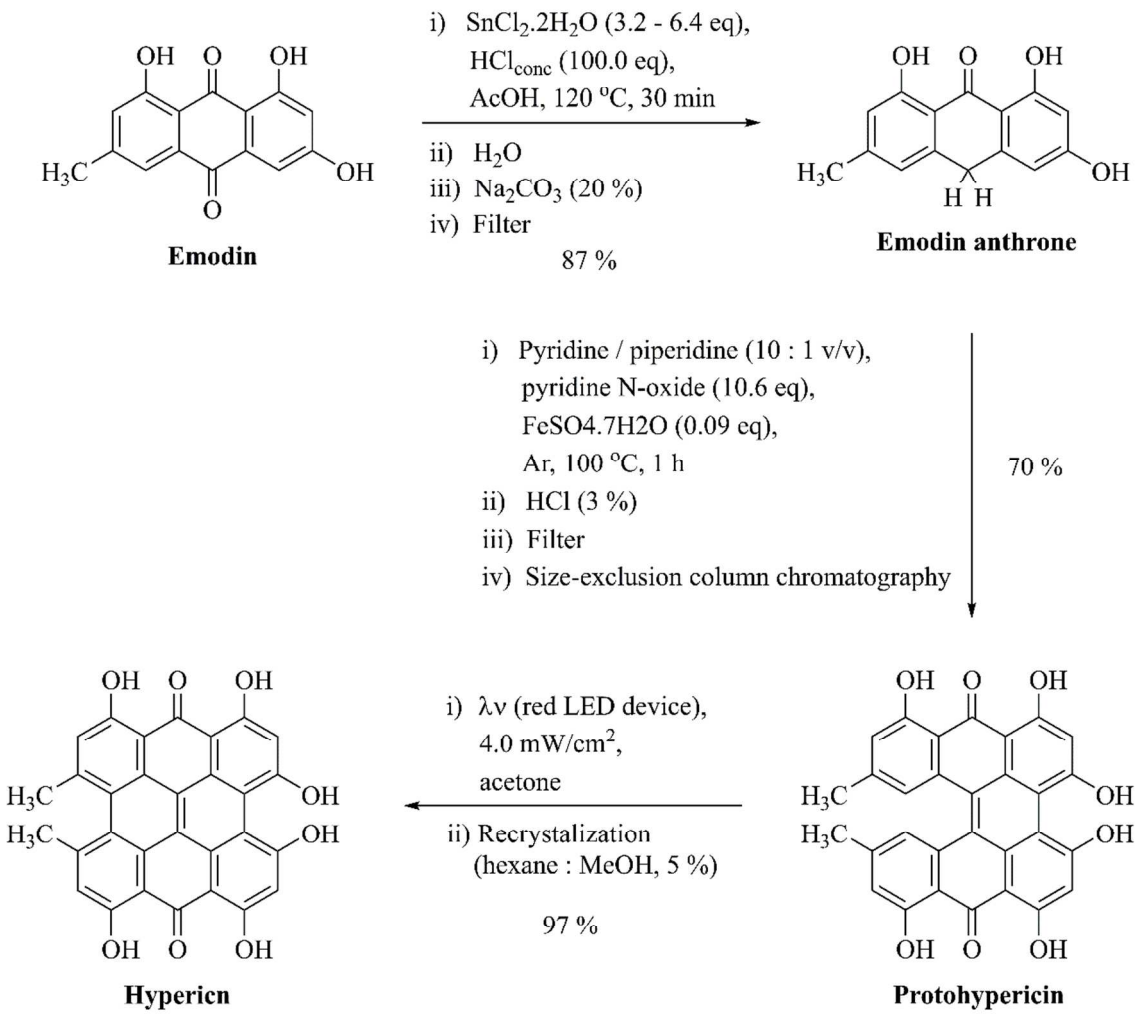


Next, the emodin was submitted to reduction reaction with tin(II) chloride dihydrate ($SnCl_2.2H_2O$) and concentrated hydrogen chloride as reducing agents to afforded the emodin anthrone. Unlike of the experimental conditions reported in the precedent works, we employed optimized reaction parameters for the emodin reduction reaction. Thus, 3.2 and 100.0 mol equiv of $SnCl_2.2H_2O$ and $HCl_{conc}$ respectively, at 120 °C for 30 min were set to converted efficiently

emodin to emodin anthrone. The crude $^{1}$H NMR analyze reveal a yield of 87% of emodin anthrone, which was used in the next step without previously purification (Figures S9-S11). Having stablished the emodin reduction reaction, we set out to synthesize protohypericin by oxidative dimerization of emodin anthrone with reproduction of the procedure reported in the patent literature.[17] Emodin anthrone was treated with a combination of pyridine N-oxide, pyridine, piperidine and ferrous sulfate at 100 $^{o}$C for 1 h to obtained the protohypericin. Although, in this precedent work the authors did not have reported a purification procedure for isolation of protohypericin from crude product, here we employed size-exclusion column chromatography and ethanol as mobile phase for yielded 70% of pure protohypericin. The $^{1}$H NMR spectroscopy analyze show a clear signature of protohypericin (Figure S12 and S13). Finally, protohypericin solution in acetone was photoconverted to hypericin with excellent yield by employing the low power red-LED photoreactor designed here, moreover the optimal LED source used for the protohypericin photoconversion was set with base on the kinetical studies showed with details in the next sessions. $^{1}$H and $^{13}$C NMR and high-resolution mass spectroscopy analysis were performed to confirm unequivocally the structure of hypericin (Figures S14-S17).

**Protohypericin Photoconversion.** The photoconversion step of the protohypericin to hypericin can be performed under irradiation with low-power light sources with well-defined spectral irradiance bands. The main advantage of this procedure in face to previous reports that use high power and multifrequential light sources is achieve the optimal experimental conditions for this step towards to multi-gram hypericin preparation process. The use of low-power light sources (LEDs) on the photoconversion stage was firstly inferred from the study published by Poutaraud et al.[32] The authors analysed empirically the influence of polychromatic light (LEDs

of the first generation) in the *in situ* photosynthesis of the pigments hypericin and pseudohypericin from St. John´s Wort and its different extracts. In this case, the optimal experimental condition observed was achieved mainly upon irradiation with green LED light source. However, for exclusive photoconversion process involving protohypericin solutions in a pure state, instead of complex plant material containing different biomolecules classes, the use of light source with different wavelength comprising the visible spectral range must be taken into account aiming to achieve the optimal experimental conditions, therefore providing more accurate information regarding specific physical-chemistry and photochemical parameters related with overall photoconversion process, on the other hands, used for the improved of the prototype photoreactor.

Aiming the optimization of the photoreaction device, in this work the multifrequential dependence on the protohypericin photocyclization reaction have been evidenced through specific experiments employing emission light sources with distinct photonic parameters. Specifically, intrinsic factors should be taken into account as wavelength emission and power LED light source, light dose, time of irradiation, prodrug concentration, and the spectral overlap between light source emission and electronic absorption spectra of protohypericin and hypericin. Moreover, the inherent effects of the hypericin photobleaching also should be relevant leading to the choice of desirable specific low-power light source. The optimized conditions for the photoconversion of protohypericin did not result in a 20% photodegradation of hypericin in the first three minutes of LED irradiation when compared to the usual light sources (mercury vapor-lamp).[17-29] Even more significantly, twenty minutes of UV exposure the hypericin show an expressive decreased of more than 90% of yield, as will be discussed below. However, the use of LED light sources enables to obtained the photoproduct in excellent yield even to a prolonged

irradiation time, overlapping the overall yield of the hypericin synthesis reported in the preceding works.

Concerning with the studies in micro scale, as a basis for photoreactor prototype design and readjustment the protohypericin photocyclization reaction kinetic profile were assessed by electronic absorption spectroscopic measurements. In a specific micro scale setup described in the Experimental Session, when an 2.0 μL protohypericin solution ($1.6 \times 10^{-5}$ mol.L$^{-1}$) is irradiated in few minutes, its initial purple color relative to the maximum absorpition band at $\lambda_{550}$ begins to turn red, concomitantly with the arising in the electronic absorption spectra of the hypericin absorption band at $\lambda_{596}$, which become more pronounced as more hypericin molecules are formed. In a first analyse, we prior investigated in micro scale the effect of the polychromatic LEDs on the protohypericin-hypericin photoconversion efficiency (Figures S1-S4). To our delight, all reactions led to excellent yields (> 97%) independently on the LED type (Table 1, entries 1-4). As earlier mentioned, the high photoconversion yields observed here are due mainly to the minimized hypericin photobleaching effect.

Table 1. Experimental conditions obtained to the protohypericin photoconversion process under different light sources.

| Entry | Conditions | Yield (%)[a] |
|---|---|---|
| 1 | Blue LED (463 nm, 10.2 mW/cm$^2$), 20 min. | 97 |
| **2** | Green LED (504 nm, 2.2 mW/cm$^2$), 28 min | 98 |
| 3 | Orange LED (593 nm, 1.0 mW/cm$^2$), 22 min | 98 |
| **4** | **Red LED (629 nm, 0.6 mW/cm$^2$), 74 min** | **Quantitative** |
| 5 | Blue LED (463 nm, 10.2 mW/cm$^2$), 800 min | 89 |
| 6 | Mercury-vapor lamp (multifrequential of 400 W), 7 min | 79 |

| | | |
|---|---|---|
| 7 | Mercury-vapor lamp (multifrequential of 400 W), 35 min | 4 |

The optimal experimental condition is indicated in bold.
[a] Yields were calculated based on epsilon values corresponding to the maximum absorption bands of protohypericin and hypericin.

The subsequent experiment where performed under long irradiation time, above of 10 hours of blue LED exposure (maximum emission at 530 nm) in order to investigated the relationship of LED sources with the hypericin photobleaching effect. The choice of this light source was made on the basis of its relatively low spectral overlap whit the main hypericin absorption band ($\lambda_{596}$), and also due to its higher light dose (10.2 mW/cm$^2$) relative to the other LEDs systems studied in this work. The Figure 2A show the electronic absorption spectra changes of the initial protohypericin solution (1.6 x $10^{-5}$ mol.L$^{-1}$) during its photoconversion to hypericin. Interestingly, the kinetic profile monitoring of the hypericin absorption band at $\lambda_{596}$ show a decrease of only 8% of absorbance, and consequently in its yield, relative to the maximum absorbance value achieved at 30 min through blue LED exposure (entry 5). This result demonstrated that the rate of the hypericin photobleaching effect is minimum relative to the time needed to reach its maximum yield irradiation with low-power LED sources.

However, at this work stage, we demonstrated the influence of the high-power multifrequential mercury-vapor lamp sources on the hypericin photobleaching effect. Thus, we performed kinetic studies of the protohypericin photoconversion with the same initial protohypericin concentration (1.6 x $10^{-5}$ mol.L$^{-1}$) similar to the previous micro-scale studies. In order to compare with the data described in the literature, we have monitored the protohypericin photoconversion via electronic absorption under mercury-vapor lamp irradiation exposure (400 W) for a reaction time of 30 min. The Figure 2B shows the complete hypericin formation at 7 min of UV exposure, in agreement with the reaction times reported in all the previous works (10-

30 min). However, at this photoreaction stage which the hypericin absorption band ($\lambda_{max}$ = 596 nm) display a maximum intensity, was observed a significant decrease of 20% in the hypericin yield in comparison with the set optimal experimental condition (compare entry 4 with 6).

Furthermore, the photobleaching effect becomes still more pronounced for UV exposure for a prolonged irradiation time (> 10 min). Under this extreme experimental condition, the hypericin molecules shown a faster photodegradation (Figure 2C), and the mainly hypericin absorption band show a decreased of 50%, visibly observed by the gradual discolored of the solution. Surprisingly, under 30 min of UV exposure, the hypericin absorption band reached a minimum value (0.19) leading a dramatic yield decrease of 96% (entry 7). This result makes it clear that the pronounced photodegradation effect becomes inevitable with the employed of high-power and multifrequential light sources on the final stage of hypericin synthesis, even for a controlled photoconversion reaction time.

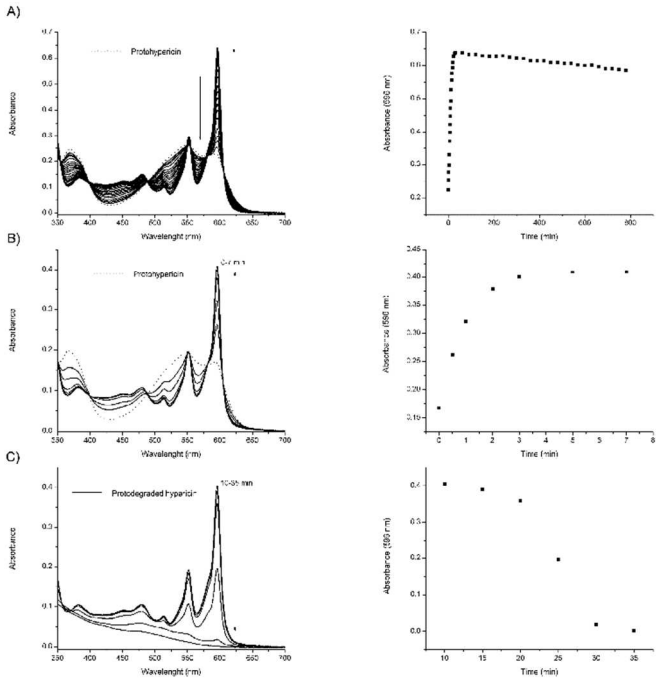


Figure 2. UV-visible kinetic monitoring of photoconversion process of the initial protohypericin solution in acetone (1.6 x $10^{-5}$ mol.$L^{-1}$). (A) Irradiation with blue LED system (10.2 mW/$cm^2$) for a reaction time of 800 min. The decreased in hypericin yield of only 11% show a photobleaching

effect practically negligible; (B) Irradiation with mercury-vapor lamp (400 W). The complete hypericin formation was accomplished at 7 min of continuous irradiation with a significant reduced yield of 79%; (C) Exceeding the irradiation time, the hypericin absorption band at $\lambda_{596}$ show a rapidly decrease and reach a minimum value after 35 min of UV exposed.

To further demonstrate the relevance of this present design, and in according with previous micro-scale studies, a gram-scale supply experiments was performed in order to evaluated the reproducibility to two low-power light sources in the preparation of the 5.0 g hypericin. To this end, we employed one photo-reactive modular unit composed of 36 SMD red or green LEDs, and the photoconversion process were monitored by real-time UV-visible spectroscopy analysis (Figures S5 and S6). The data showed a high-efficiency photoconversion to both LEDs systems, and with reproducibility of the optimized experimental conditions set in micro-scale (Table 2). The red-LED photoreactor was employed to photoconverted quantitatively an initial $3.3 \times 10^{-3}$ $mol.L^{-1}$ protohypericin concentration to hypericin, after 8 cycles of continuous irradiation with a 4.0 $mW/cm^2$ light dose. However, only 3 cycles of continuous irradiation with the green-LED photoreactor of 11.3 $mW/cm^2$ light dose, were necessary to the complete photoconversion of the same protohypericin concentration, yielding 98% of hypericin, i.e. an irradiation time of approximately 2.7 times lower than that obtained for the red-LED system. The high spectral overlap of the green LED whit the main hypericin absorption band ($\lambda_{596}$) lead to a possible photobleaching effect, which results in this small difference in the hypericin yield observed between the two LEDs systems. Consequently, on one hand the employ of the green-LED photoreactor in the production of hypericin in industrial scale could resulted in a significative reduction of the energy consumption, but on the other, possible yield losses inherent to the photodegradation process would inevitably lead to an increasing of final cost. From this point of view independently of the LED light system used in the production of hypericin, the significant

benefits of the present design in comparison with the usual mercury-vapor lamps, involve mainly the higher-efficient in the protohypericin-hypericin photoconversion process. Additionally, the optimization of the photonic parameters demonstrated here allows to achieved a safe and reproductive scale-up protocol for the hypericin synthesis with a lower power consumption, and higher yield. Finally, although in this work we demonstrated the high efficiency of the LED based photoreactor for a gram-scale supply of hypericin, the innovative flow continuously system designed for this prototype allow that the hypericin can be prepared in a scale even higher overcoming the limitations related to open irradiation systems previously reported, which require a wide contact surface between the protohypericin solution and the irradiation light source, limiting the large-scale production of hypericin.

Table 2. Experimental conditions obtained to the protohypericin photoconversion process under red and green-LED photoreactors.

| LED photoreactor | Wavelength (nm) | Light dose ($mW/cm^2$) | Number of cycles | Reaction time (min) | Isolated yields (%) | Comments |
|---|---|---|---|---|---|---|
| Red | 629 | 4.0 | 8 | 13,6 | **Quantitative** | Low spectral overlap with hypericin |
| Green | 504 | 11.3 | 3 | 5,1 | 98 | High spectral overlap with hypericin: Possible photobleaching |

## CONCLUSIONS

This work presents an improved synthesis process developed for a multigram production of hypericin. The main problem presented in such process resides in a low yield and purity degree hypericin production implying to high commercial cost of the final product. Therefore, in order to optimize the overall hypericin process, especially concerning with its critical final stage related with the protohypericin photocyclization reaction, an inexpensive and efficient low power

Light Emission Diode (LED) based photoreactor was also designed. Taking into account the suitable photonic parameters like the wavelength emission and power LED light source, light dose, time of irradiation, pro-drug concentration, and the spectral overlap overcoming, the undesirable intrinsic hypericin photobleaching effect, and hypericin multigram synthesis can be achieving in excellent yields nearby 98% for all kind of LEDs, dependent on all of these photonic parameters. Finally, this closed system also overcomes safety issues related to scale-up hypericin preparation typically described in the literature which combine the use of open systems, organic solvents and high-power light sources. Furthermore, this system can be applied to other photoreaction systems.

## EXPERIMENTAL SECTION

**Materials.** Reactants and reagents were purchased from commercial sources and used without further purification, except for emodin, which was isolated from *Cortex Frangula*.[34]

**Experimental Methods**. Nuclear magnetic resonance spectra were recorded on a Bruker AVANCE III HD 500 MHz spectrometer operating respectively at 500,133 and 125,03 MHz, equipped with direct field gradient and probe of 5 mm, and at a constant temperature of 25$^{o}$ C. All samples were prepared with an addition of 0.7 mL of deuterated solvents in 5-10 mg of compounds. $^{1}$H and $^{13}$C NMR data are recorded in DMSO-$d_6$, and $CD_3CN$ listed as residual internal: DMSO-$d_5$ (δ 2.50 and 40.0), $CD_2HCN$ (δ 1.39) and the spectra were referenced as the TMS peak. Data are presented as follows: chemical shift (ppm), multiplicity (s = singlet, d = doublet, dd = doublet of doublet, dq = doublet of quartet), and integration. All spectra were processed using the Bruker TopSpin 3.1 software. High resolution mass spectroscopy spectrum was recorded by direct infusion ESI-MS on a hybrid quadrupole orthogonal time-of-flight mass

spectrometer, QTof HRMS (Waters Corporation, Milford, MA, USA), controlled by MassLynx 4.1 software. The electrospray ionization was performed in the negative ion mode (ESI-) with capillary voltage set to 2.5 kV, cone voltage to 35 V and source temperature to 150 ºC. The desolvation gas was nitrogen, with flow of 700 L $h^{-1}$ and temperature of 400 °C. Data was acquired from *m/z* 50 to 1000 in MS mode and $MS^2$ experiment was acquired from *m/z* 50 to 600, in which the collision energy alternated between low energy (2 V) and high energy (45 V). Leucine-enkephalin (Waters Corporation, USA), $C_{28}H_{35}N_5O_7$ ($[M-H]^-$ of *m/z* 554.2771) was used as reference at a concentration of 0.2 ng $L^{-1}$.

Electronic absorption spectroscopy analysis (UV-visible) were recorded on a Beckman Coulter DU800 UV-visible Spectrophotometer at room temperature. Protohypericin photocyclization kinetics analysis were measured through UV-visible analysis. Aliquots of protohypericin in acetone ($1.6 \times 10^{-5}$ mol.$L^{-1}$) were added in quartz cuvettes with a 1 cm optical pathway. The cuvettes were fixed in a support adapted with six lateral LEDs (three in each lateral), arranged at 0.5 cm of the solution.[33] The experiments were performed with four groups of low-power 1210-SMD LEDs sources: Blue, green, orange, and red (0.6 – 10.2 mW/$cm^2$). The absolute irradiance of LEDs was measured using an *Ocean Optics* spectrometer, model USB4000-UV-VIS.

**Procedure for the synthesis of emodin anthrone.** For a suspension of emodin (10.0 g, 37.0 mmol), in acetic acid (350 mL) kept in a round-bottom flask, a solution of $SnCl_2.2H_2O$ (52.3 g, 0.22 mmol) in $HCl_{conc}$ (365 mL, 370 mmol) was added and the solution was heated to 120 $^oC$ for 30 min under vigorous stirring. The solution was cooled, poured in water (2 L) and neutralized with $Na_2CO_3$. The precipitate was filtered off, washed with distilled water and drying under vacuum to yield 8.7 g (87%) of yellow/brown solid. $C_{15}H_{12}O_4$, $^1H$ NMR (DMSO-$d_6$, 25 $^oC$, 500

MHz): $\delta_H$ 12.37 (s, 1H, OH-1), 12.21 (s, 1H, OH-8), 10.84 (s, 1H, OH-3), 6,77 (m, 1H, *Ar*-H4), 6.67 (m, 1H, *Ar*-H5), 6.42 (dq, 1H, *Ar*-H2), 6.23 (d, 1H, *Ar*-H7), 4.30 (s, 2H, *Benz*-H10), 2.32 (dd, 3H, *Ar*-$CH_3$) ppm; $^{13}$C NMR (DMSO-$d_6$, 25 $^{o}$C, 75 MHz): $\delta_C$ 191.35 (-C=O), 165.24 (C6), 164.81 (C8), 161.91 (C1), 147.32 (C11), 145.23 (C14), 142.25 (C13), 120.15 (C4), 115.39 (C3), 113.08 (C12), 108.65 (C2), 107.64 (C5), 101.23 (C7), 32.51 (C9), 21.84 (-$CH_3$); UV-Vis (EtOH) $\lambda_{max}$ 250, 258, 271, 300 e 353 nm. The characterization data of emodin anthrone are in agreement with the literature.[35]

**Procedure for the synthesis of protohypericin.** To a solution of emodin anthrone (8.00 g, 31.2 mmol) in 176 mL of pyridine/piperidine (10:1 v/v), were added 16.0 g (168 mmol) of pyridine N-oxide and 0.4 g of ferrous sulphate heptahydrate (1.44 mmol) and the mixture was heated in the dark at 100 $^{o}$C for 1 h under vigorous stirring. After cooling, the solvent was concentrated to approximately 5.0 mL and the solution was neutralized with 3% HCl solution. The precipitate was filtered off, washed with water and then dried under vacuum for 24 h. Crude product was purified by size-exclusion column chromatography (SEC) using Sephadex® LH-20 matrix and EtOH as mobile phase to yield 5.60 g (70%) purple crystals. $C_{30}H_{18}O_8$; $^1$H NMR (DMSO-$d_6$, 25 $^{o}$C, 500 MHz): $\delta_H$ 14.40 (s, 2H, OH-1, OH-6), 12.89 (s, 2H, OH-7, OH-14), 7.24 (s, 2H, *Ar*-H8, *Ar*-H13), 6.78 (s, 2H, *Ar*-H10, *Ar*-H11), 6.33 (s, 2H, *Ar*-H2, *Ar*-H5), 2.09 (s, 6H, *Ar*-$CH_3$) ppm; UV-Vis (EtOH) $\lambda_{max}$ 369, 524 e 596 nm.

**Procedure for the synthesis of hypericin.** Protohypericin solution (5.00 g, 9.85 mmol) in acetone (3 L) was charged into 5 L feed amber flask and pumped into the flow cell by down of the photoreactor at a volumetric flow rate (1.25 x $10^{-4}$ $m^3/s$). The solution was irradiated with four photo-reactive modular units vertically arranged in series, each one composed by 36 x red 1210-SMD (Surface Mounted Diode) LEDs of light dose 12.5 mW/$cm^2$ (Honglitronic). The rate

photoconversion was monitored until the hypericin absorption band at $\lambda_{596}$ nm reached a maximum of intensity, correspondent with a quantitative photoconversion of protohypericin to hypericin. The crude product was recrystallized from a mixture of hexane : MeOH (95:5 v/v) to afford an blue-dark crystalline solid. Yield: 4.85 g, 97%. $C_{30}H_{16}O_8$; $^1$H NMR ($CD_3CN$, 25 $^oC$, 500 MHz): $\delta_H$ 14.75 (s, 2H, OH-1, OH-6), 14.13 (s, 2H, OH-7, OH-12), 7.31 (s, 2H, *Ar*-H8, *Ar*-H11), 6.55 (s, 2H, *Ar*-H2, *Ar*-H5), 2.71 (s, 6H, *Ar*-$CH_3$) ppm; UV-Vis (EtOH) $\lambda_{max}$ 392, 480, 513, 552, 596. $^{13}$C NMR ($CD_3CN$, 25 $^oC$, 500 MHz): $\delta_C$ 185.2, 175.7, 169.8, 162.8, 144.6, 128.4, 127.6, 122.7, 122.1, 120.5, 119.6, 109.9, 106.6, 103.5. The identification of molecular formula of Hypericin ($C_{30}H_{16}O_8$) was confirmed on its negative HRMS ion of *m/z* 503,0854 (calcd for $[M- H]^-$ 503,0845). The $MS^2$ experiment showed fragments ions characteristic for this compound of *m/z* 487.0202 $[M- H- CH_4]^-$, 458.0504 $[M- H- CO_2- H\cdot]^-$, 433.0361 $[M- H- CH_2=C=O- CO]^-$, 431.0601 $[M- H- CO_2- CO]^-$ and 405.0425 $[M- H- CH_2=C=O- 2CO]^-$. The characterization data of hypericin are in agreement with the literature.[35-39]

## ASSOCIATED CONTENT

## AUTHOR INFORMATION

### Corresponding Author

*email: rsgoncalves2@uem.br

### Notes

The authors declare no competing financial interest.

### Funding Sources

Fundação Araucária/PR, CNPQ (p 308142/2014□4), CAPES

**Supporting Information Available.**

Experimental procedures, characterization data and copies of spectra are available free for charge via the Internet at

## REFERENCES

1. Karioti, A.; Bilia, A. R. *Int. J. Mol. Sci*. **2010**, *11*, 562-594.
2. Joniova, J.; Rebic, M.; Strejckova, A.; Huntosova, V.; Stanicova, J.; Jancura, D.; Miskovsky, P.; Bano, G. *Biophys. J.* **2017**, *112*, 966-975.
3. Do, M. H.; Kim, S. Y. *Biomol. Ther.* **2017,** *25*, 158-164.
4. Huntosova, V.; Novotova, M.; Nichtova, Z.; Balogova, L.; Maslanakova, M.; Petrovajova, D.; Stroffekova, K. *Toxicol. In Vitro* **2017**, *40*, 184-195.
5. Brockmann, H. *Angew. Chem.* **1949**, *61*, 389-389.
6. Brockmann, H. *Chem. Ber./Recl.* **1949**, *82*, 348-357.
7. Brockmann, H.; Kluge, F. *Naturwissenschaften* **1951**, *38*, 141-141.
8. Brockmann, H.; Neeff, R. *Naturwissenschaften* **1951**, *38*, 47-47.
9. Brockmann, H.; Sanne, W. *Naturwissenschaften* **1953**, *40*, 461-461.
10. Brockmann, H.; Eggers, H. *Angew. Chem., Int. Ed. Engl.* **1955**, *67*, 706.
11. Brockmann, H.; Eggers, H. *Angew. Chem., Int. Ed.* **1955**, *67*, 706-706.
12. Brockmann, H.; Kluge, F.; Muxfeldt, H. *Chem. Ber./Recl.* **1957**, *90*, 2302-2318.
13. Brockmann, H.; Eggers, H. *Chem. Ber./Recl.* **1958**, *91*, 81-100.
14. Steglich, W.; Arnold, R. *Angew. Chem., Int. Ed. Engl.* **1973**, *12*, 79-79.
15. Banks, H. J.; Cameron, D. W.; Raverty, W. D. *Aust. J. Chem.* **1976**, *29*, 1509-1521.
16. Rodewald, G.; Arnold, R.; Griesler, J.; Steglich, W. *Angew. Chem., Int. Ed. Engl.* **1977**, *16*, 46-47.
17. Mazur Y.; Bock H.; Lavie D. CA 2 029 993. **1989**.
18. Falk, H.; Schoppel, G. *Monatsh. Chem*. **1992**, *123*, 931-938.
19. Falk, H.; Meyer, J.; Oberreiter, M. *Monatsh. Chem*. **1993**, *124*, 339-341.
20. Kraus, G. A.; Zhang, W. *Bioorg. Med. Chem. Lett.* **1995**, *5*, 2633-2636.
21. Falk, H.; Vaisburg, A. F.; Amer, A. M. *Monatsh. Chem*.**1995**, *126*, 993-1000.
22. Falk, H.; Sarhan, A.; Tran, H. T. N.; Altmann, R. *Monatsh. Chem*. **1998**, *129*, 309-318.
23. Altmann, R.; Falk, H.; Gruber, H. J. *Monatsh. Chem*. **1998**, *129*, 235-244.
24. Kowalik, E. G.; Zalkow, L. H. *Org. Prep. Prep. Proced. Int.* **2000**, *32*, 57-61.
25. Kim, S. W.; Park, J. H.; Yang, S. D.; Hur, M. G.; Kim, Y.; Chai, J.; Kim, Y. S.; Yu, K. H. *Bull. Korean Chem. Soc.* **2004**, *25*, 1147-1150.
26. Motoyoshiya, J.; Masue, Y.; Nishi, Y.; Aoyama, H. *Nat. Prod. Comm*. **2007**, *2*, 67-70.
27. Falk, H. *Monatch. Chem.* **2008**, *139*, 991-993.
28. Tobia, A. J.; Cabana, B. E.; Vadlapatla, V.; Connolly, R. H. US20120245392A1. **2012**.

29. Fang, H.; Hui, W.; Lin, C. *Chin. J. Nat. Med.* **2014**, *12*, 81-88.
30. Serra, F.; Terentjev, E. M. *J. Chem. Phys*. **2008**, *128*, 6.
31. Uzdensky, A. B.; Iani, V.; Ma, L. W.; Moan, J. *J. Photochem. Photobiol*., A **2002**, *76*, 320-328.
32. Poutaraud, A.; Di Gregorio, F.; Tin, V.C.F.; Girardin, P. *Planta Med*. **2001**, *67*, 254-259.
33. Rabello, B. R.; Gerola, A. P.; Pellosi, D. S.; Tessaro, A. L.; Aparicio, J. L.; Caetano, W.; Hioka, N. *J. Photochem. Photobiol*., *A* **2012**, *238*, 53-62.
34. Gonçalves, R.S; Silva, L.E.; Hioka, N.; Nakamura, C.V.; Bruschi, M.L.; Caetano, W. *Nat. Prod. Res.* **2017**, 1-4.
35. Kapinus, E. I.; Falk, H.; Tran, H. T. N. *Monatch. Chem.* **1999**, *130*, 623-635.
36. Piperopoulos, G.; Lotz, R.; Wixforth, A.; Schmierer, T.; Zeller, K-P. *J. Chromatogr. B*. **1997**, *695*, 309-316.
37. Brolis, M.; Gabetta, B.; Fuzzati, N.; Pace, R.; Panzeri, F.; Peterlongo, F. *J. Chromatogr. A.* **1998**, *825*, 9-16.
38. Riedel, K-D.; Rieger, K.; Martin-Facklam, M.; Mikus, G.; Haefeli, W. E.; Burhenne, J. *J. Chromatogr. B*. **2004**, *813*, 27-33.
39. Gadzovska, S.; Maury, S.; Ounnar, S.; Righezza, M.; Kascakova, S.; Refregiers, M.; Spasenoski, M.; Joseph, C.; Hagège, D. *Plant Physiol. Biochem.* **2005**, *43*, 591-601.

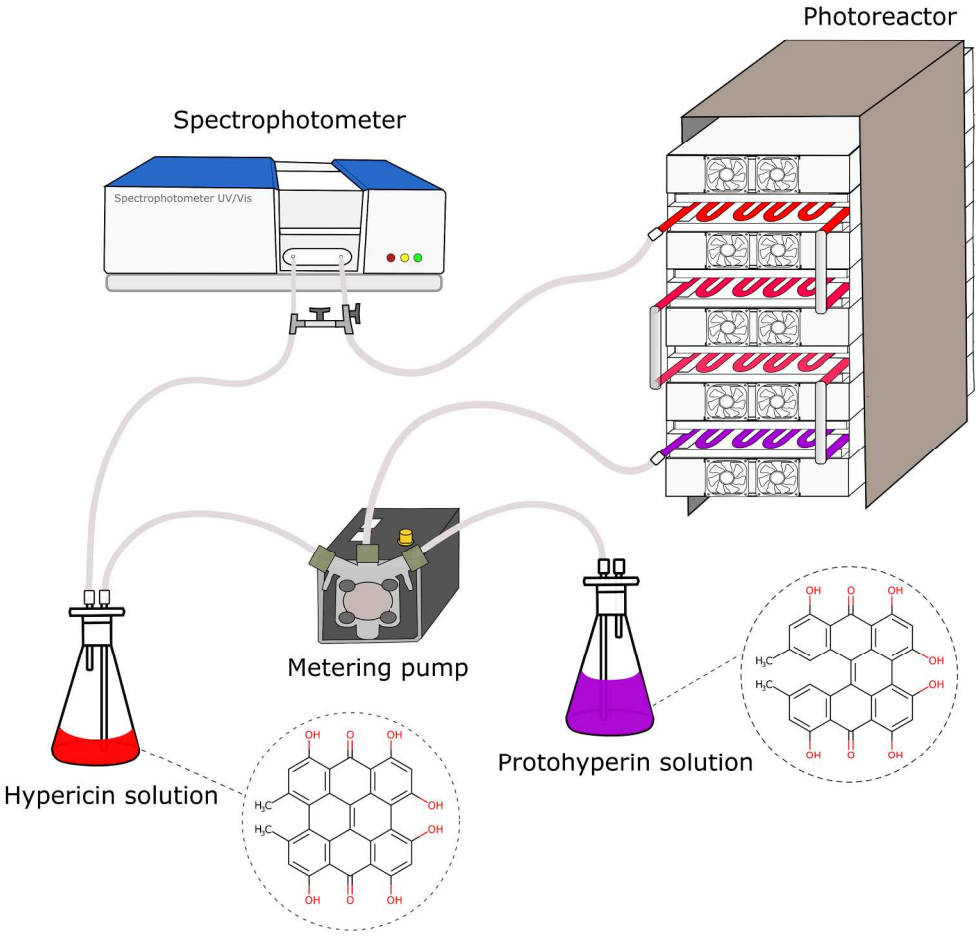


TOC graphic

109x112mm (600 x 600 DPI)

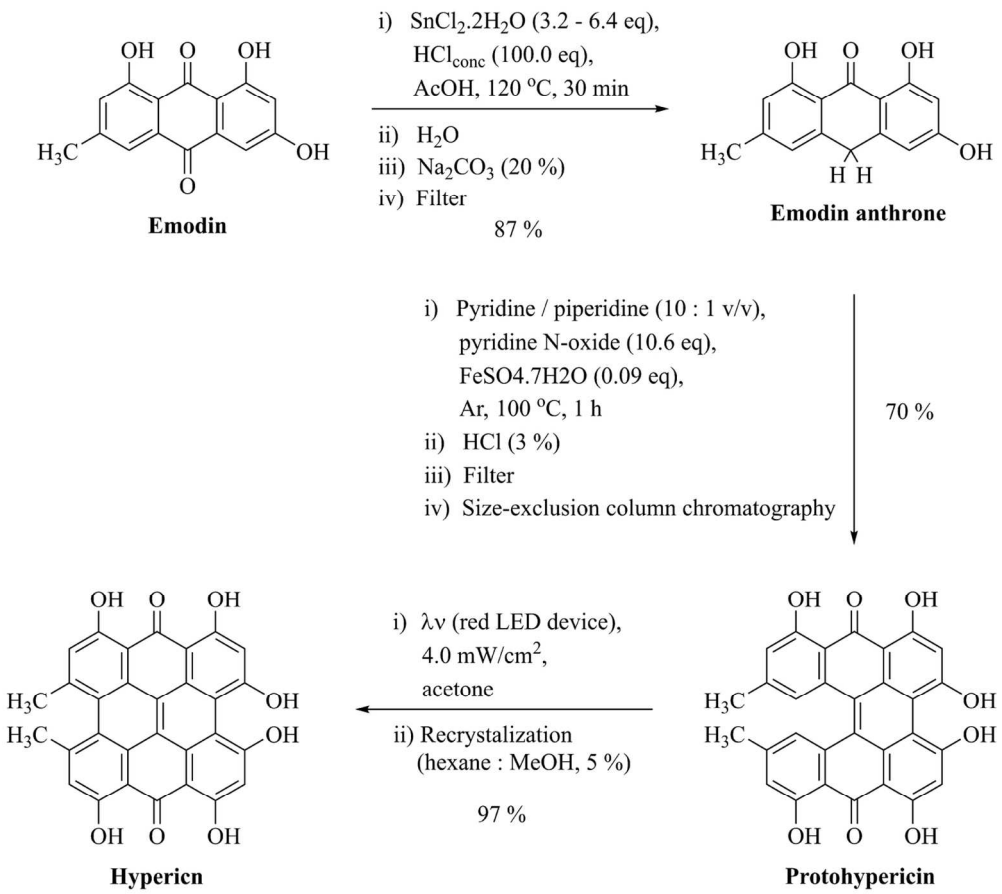


Scheme 1. Optimized experimental conditions for the hypericin synthesis.

63x56mm (600 x 600 DPI)

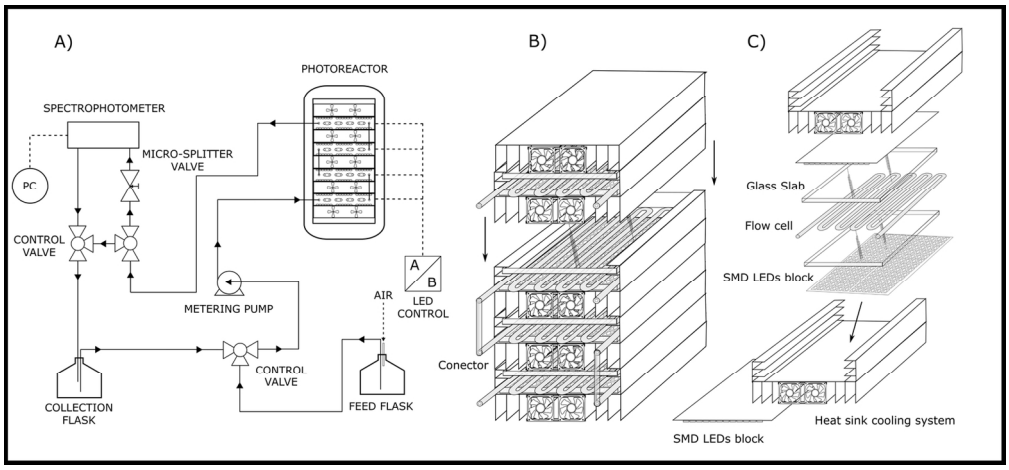


Figure 1. (A) Process flow diagram of the protohypericin photoconversion. (B) Showing the photoreactor vertically arranged with four photo-reactive modular units interlocked. (C) Showing the deconstructed modular unit. The flow cell is inserted between two glass slabs preventing the intimate contact of the sample with the irradiation systems.

71x32mm (600 x 600 DPI)

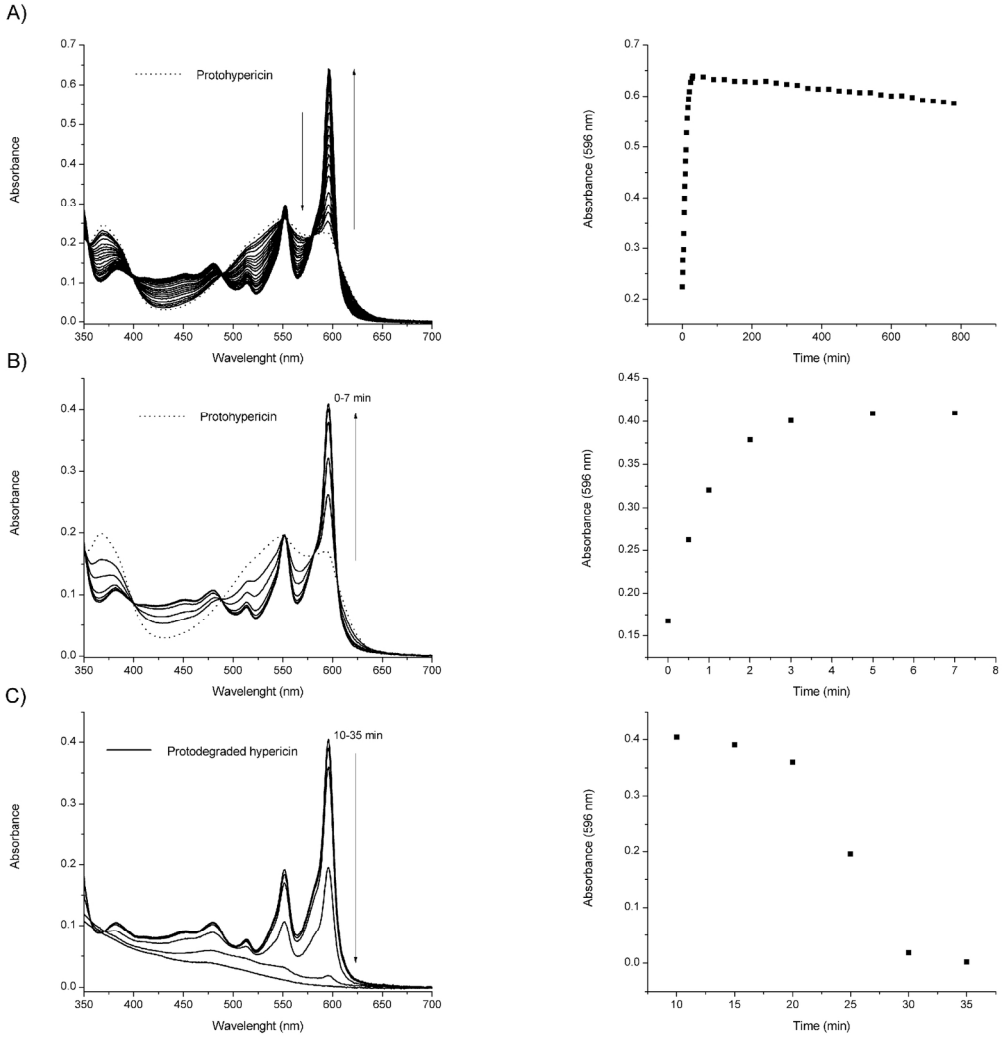


Figure 2. UV-visible kinetic monitoring of photoconversion process of the initially protohypericin solution in acetone ($1.6 \times 10^{-5}$ mol.L$^{-1}$). (A) Irradiation with blue LED system (10.2 mW/cm$^2$) for a reaction time of 800 min. The decreased in hypericin yield of only 11 % show a photobleaching effect practically negligible; (B) Irradiation with mercury-vapor lamp (400 W). The complete hypericin formation was accomplished at 7 min of continuous irradiation with a significant reduced yield of 79%; (C) Exceeding the irradiation time, the hypericin absorption band at $\lambda_{596}$ show a rapidly decrease and reach a minimum value after 35 min of UV exposed.

89x92mm (600 x 600 DPI)